DOI: 10.1038/ncb3036

nature cell biology

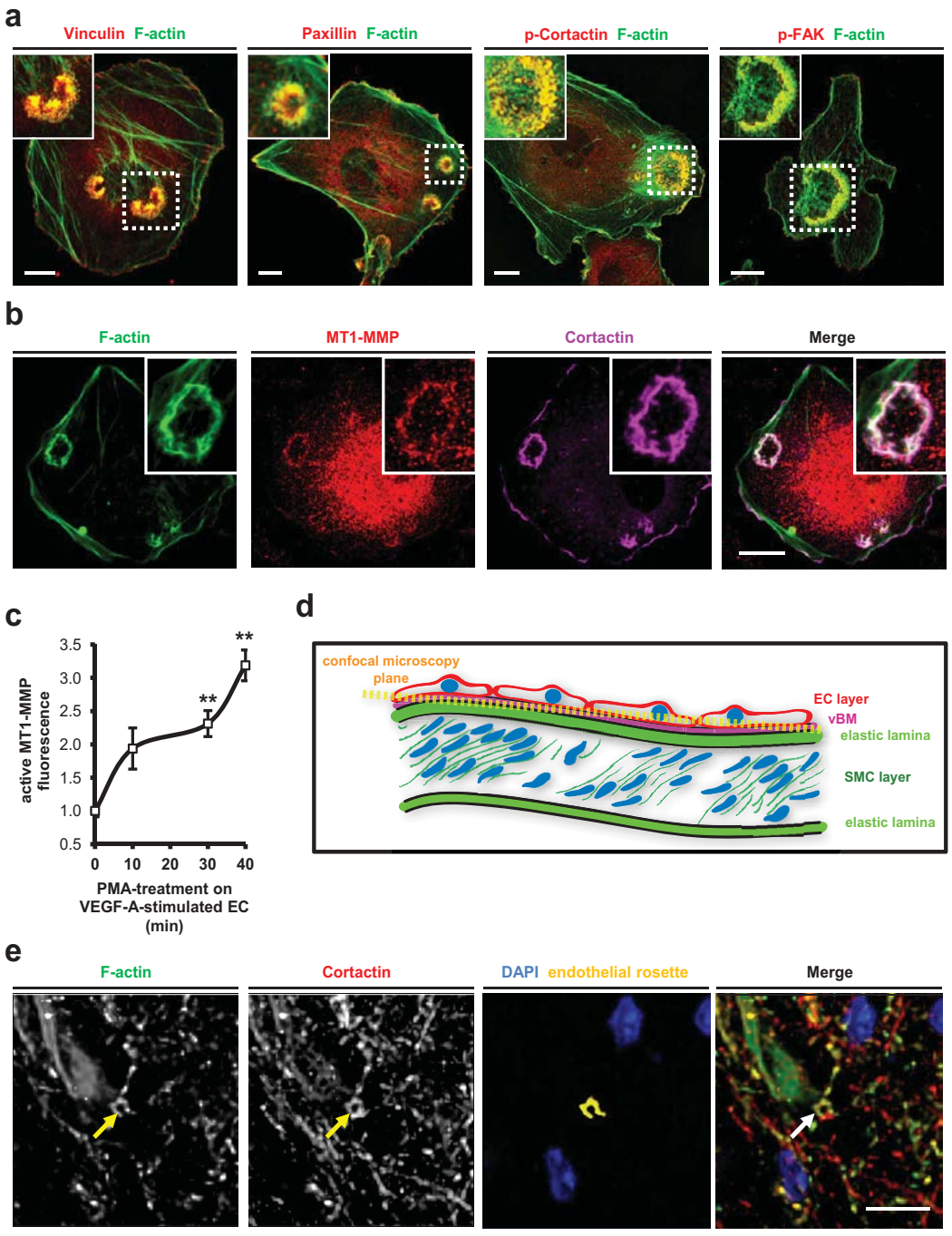

Supplementary Figure 1 Endothelial podosome rosettes in cultured EC and aortic explants. (**a-b**) Immunostained representative VEGF-A-stimulated EC treated with PMA for 30 min. Scale bar: 10 µm. (**c**) Cytofluorimetric analysis of membrane MT1-MMP localization. EC treated with PMA for the indicated time. Normalized mean ± SEM of n = 3 independent experiments in which 8×10^4 cells were analyzed per experimental point. (**, P < 0.01 versus *T=0*.) Statistical significance was calculated using paired nonparametric Wilconox test. (**d**) Schematic representation of mouse aortic explant micro-anatomy. Endothelial cells (EC) are characterized by large round nuclei and vascular smooth muscle cells (SMC) by thin and elongated nuclei. Along the z-axis, the two cell types were seen separated by the top elastic lamina. Yellow dotted line, schematization of the *z* plane of microscopic analysis of endothelial rosettes. (**e**) Immunostaining of a representative 48 h VEGF-A-stimulated aortic explant. In yellow, 3D reconstruction of the co-localization channel in podosome rosette. Individual channel images from Fig. 1e. Scale bar: 20 µm.

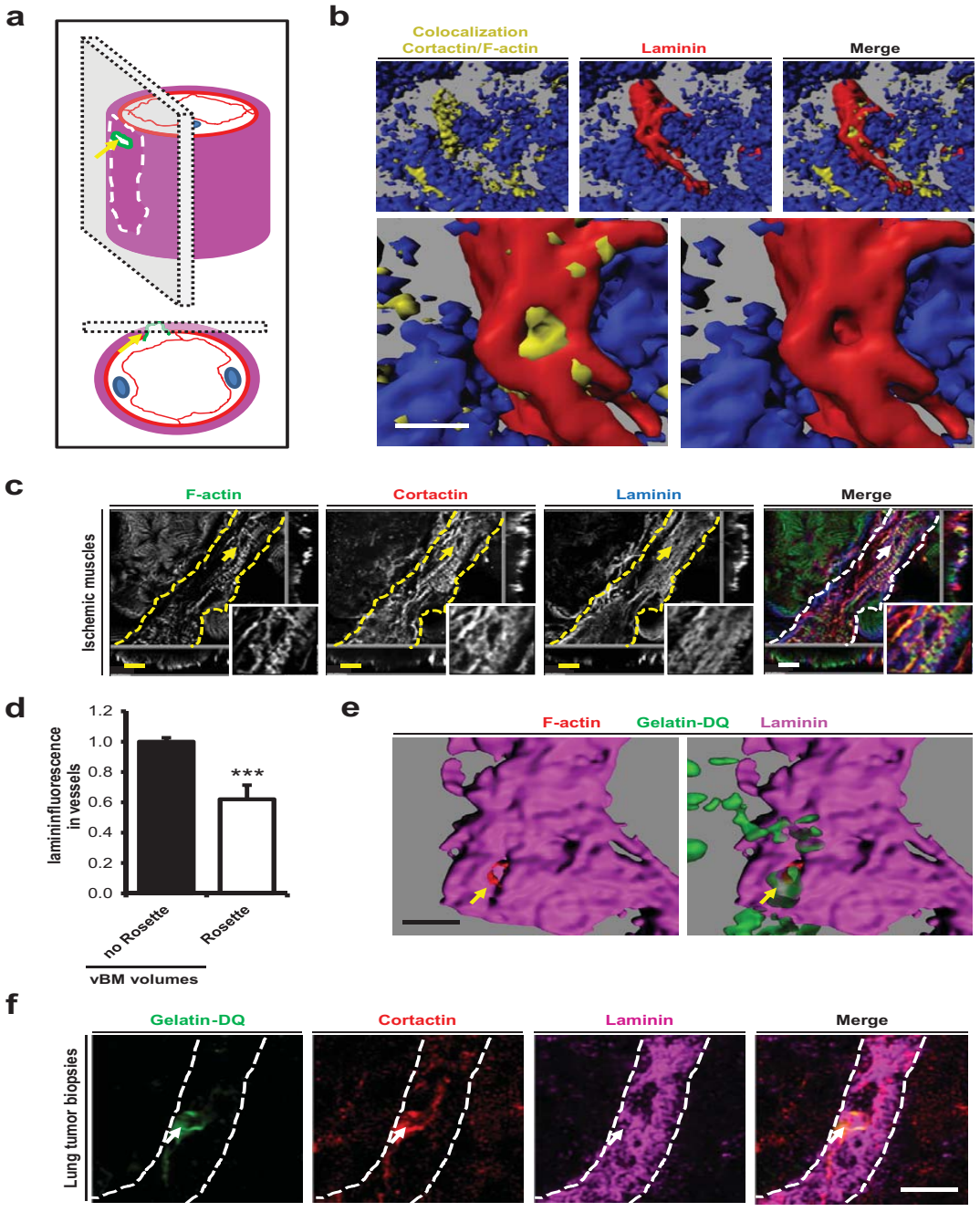

Supplementary Figure 2 3D rendering of endothelial podosome rosettes in RipTag2 tumour and ischaemic vessels. (**a**) Schematic representation of endothelial tumoural rosettes detection. Endothelial cells (EC) are delimited by red line while vBM is colored in magenta, in green there is the schematization of endothelial tumoural rosettes visualized as shown in Fig. 2a. Yellow arrows indicate the rosettes. (**b**) 3D reconstruction of a representative endothelial rosette in RipTag2 tumours. Isosurface of vBM – detected as laminin staining – was coloured in red, endothelial rosettes – F-actin/cortactin co-localization – in yellow and nuclear staining in blue. Scale bar: 5 µm. (**c**) Confocal imaging stacks of representative vessels in hindlimb ischaemia experiment on gastrocnemius muscles. *Xyz*-section of immunostaining for primary Abs as indicated. Vessels are delimited by white dotted lines; white arrows indicate podosome-rosettes. Scale bar: 10 µm. (**d**) vBM quantification in different regions of tumour vessels in RipTag2 tumours. vBM was detected as laminin staining. vBM volumes were subdivided in 1000-µm^3-volumes. Therefore, the sub-volumes of vBM were classified in vBM volumes without endothelial rosettes (*no rosette vBM volumes*) and vBM volumes with endothelial rosettes (*rosette vBM volumes.*) Normalized mean ± SEM of n = 420 subvolumes of vBM from 5 fields per mouse for a total of 3 mice per treatment group. (***, $P < 0.001$ versus *no rosette vBM volumes.*) Statistical significance was calculated using unpaired nonparametric Mann-Whitney test. (**e**) 3D reconstruction of *in situ* zymography in a representative endothelial rosette of RipTag2 tumours. After deconvolution, isosurface of vBM – detected as laminin staining – was coloured in magenta, F-actin in red and Gelatin-DQ – indication of gelatin degradation – in green. Scale bar: 10 µm. (**f**) *In situ* zymography in lung tumours from patients. Staining for primary Abs as indicated and Gelatin-DQ (dye-quenched), *i.e.* degradated gelatin. Vessel is delimited by white dotted lines; white arrows indicate podosome-rosettes. Scale bar: 10 µm.

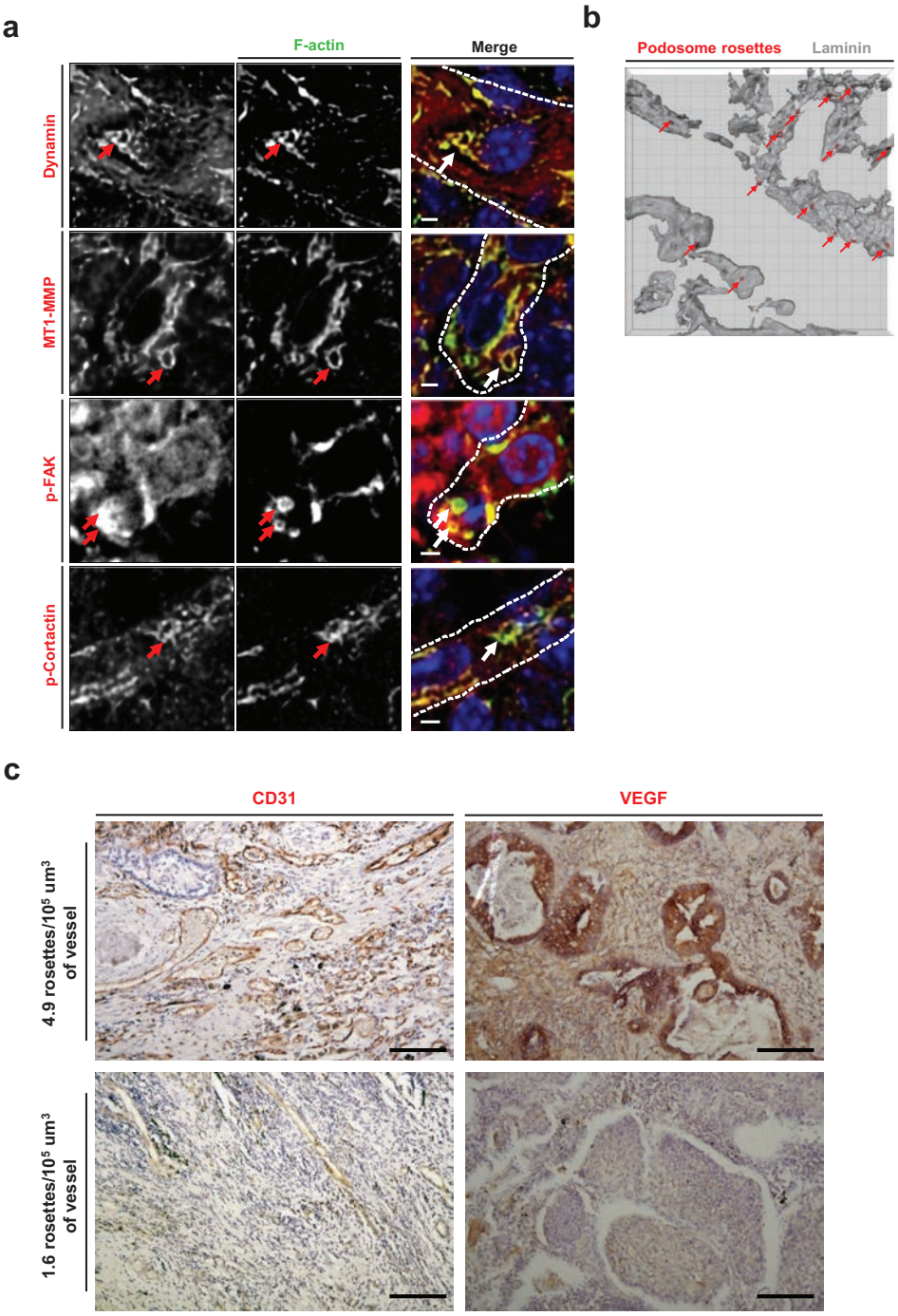

Supplementary Figure 3 Endothelial podosome markers and endothelial density in tumours vessels. (**a**) Confocal images of representative vessels in angiogenic islets of RipTag2 mice. *Xyz*-section of immunostaining for primary Abs as indicated and nuclear-stained by DAPI (blue). Vessels are delimited by white dotted lines; white arrows indicate podosome-rosettes. Scale bar: 3 µm. (**b**) 3D isosurface rendering of tumour vessels in a 12-µm-thick slice of a representative RipTag2 angiogenic islet. Vessels (gray) detected with laminin staining and podosome-rosettes (red) recognized with co-localization of F-actin/cortactin staining. Red arrows indicate podosome-rosettes. Tickmarks on axis: 10 µm. (**c**) Representative micrograph images of CD31 and VEGF staining in biopsy samples of lung tumours. Scale bar: 50 µm. Quantifications and correlations in Fig. 2d.

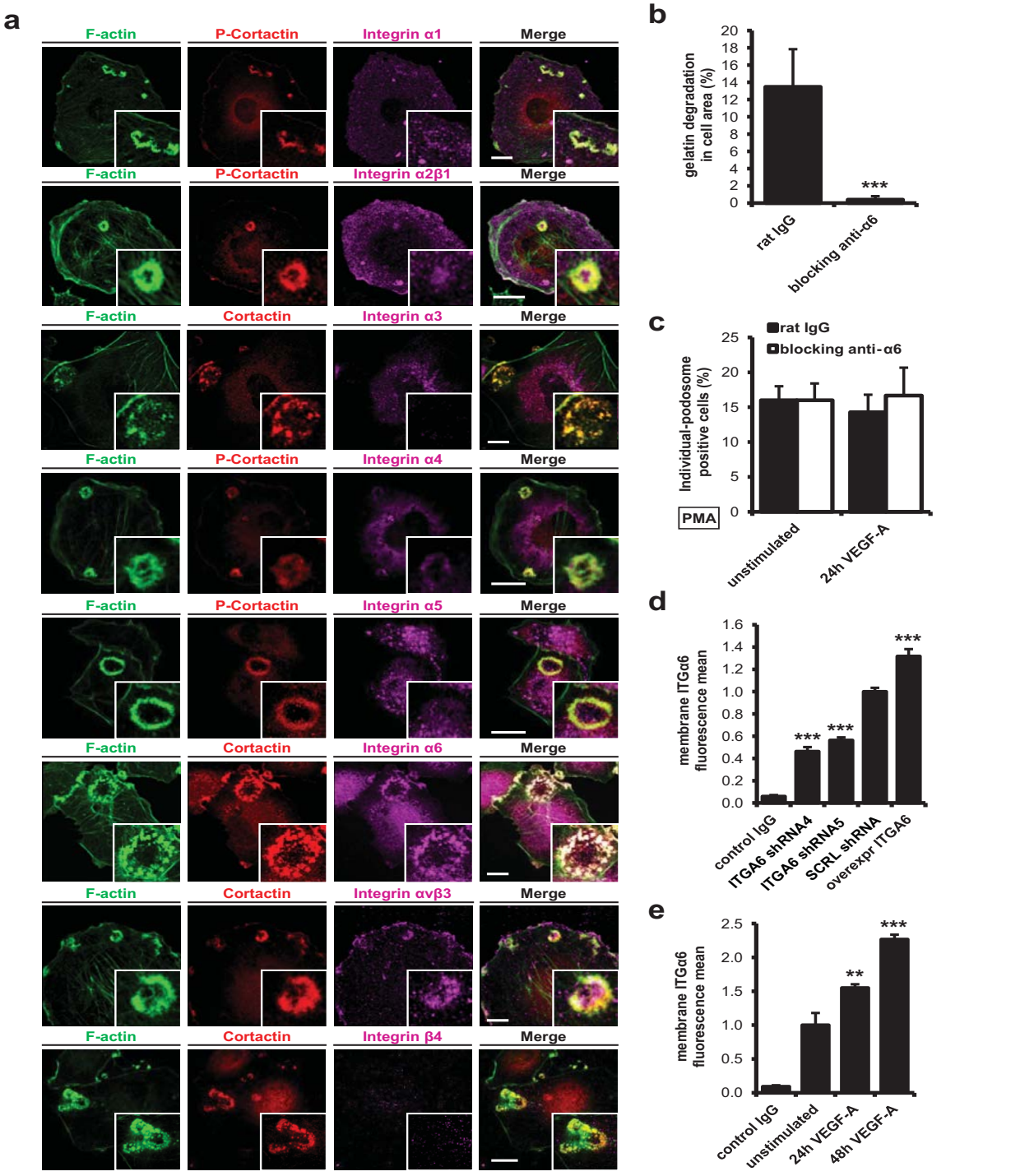

Supplementary Figure 4 Integrin recruitment in endothelial podosome rosettes. (**a**) Confocal images of representative VEGF-stimulated EC, PMA-treated for 30 min. Inset, of the podosome-rosettes. Scale bar: 20 μm. (**b**) Gelatin degradation assay on EC treated with rat IgG or anti-α6 blocking Ab after 1 hour of stimulation with PMA. Mean ± SEM of n = 10 cells from 3 independent experiments (***, P < 0.001 versus *Rat IgG*.) Statistical significance was calculated using unpaired nonparametric Mann-Whitney test. (**c**) Graph shows the percentages of individual podosome positive EC, stimulated as indicated and treated with rat IgG or anti-α6 blocking Ab. Mean ± SEM of n = 3 independent experiments in which 250 total cells were analyzed cells per experimental point. (**d**) Cytofluorimetric analysis of membrane integrin α6 localization. EC were transduced with shRNA scramble (*SCRL shRNA*) or against integrin α6 (*ITGA6 shRNA4* and *shRNA5*). Mean ± SEM of n = 3 independent experiments (***, P < 0.001 versus *shSCRL*.) Statistical significance was calculated using one-way ANOVA test followed by Bonferroni adjusted post-hoc t-tests. (**e**) Cytofluorimetric analysis of membrane integrin α6 localization. EC were incubated for 24 h in M199 10% FCS (*unstimulated*) or in M199 10% FCS plus 30 ng/ml of VEGF-A (*24 h VEGF-A*) or for 48 h in M199 10% FCS plus 30 ng/ml of VEGF-A (*48 h VEGF-A*). Mean ± SEM of n = 3 independent experiments. (**, P < 0.01 versus *unstimulated*; ***, P < 0.001.) Statistical significance was calculated using one-way ANOVA test followed by Bonferroni adjusted post-hoc t-tests.

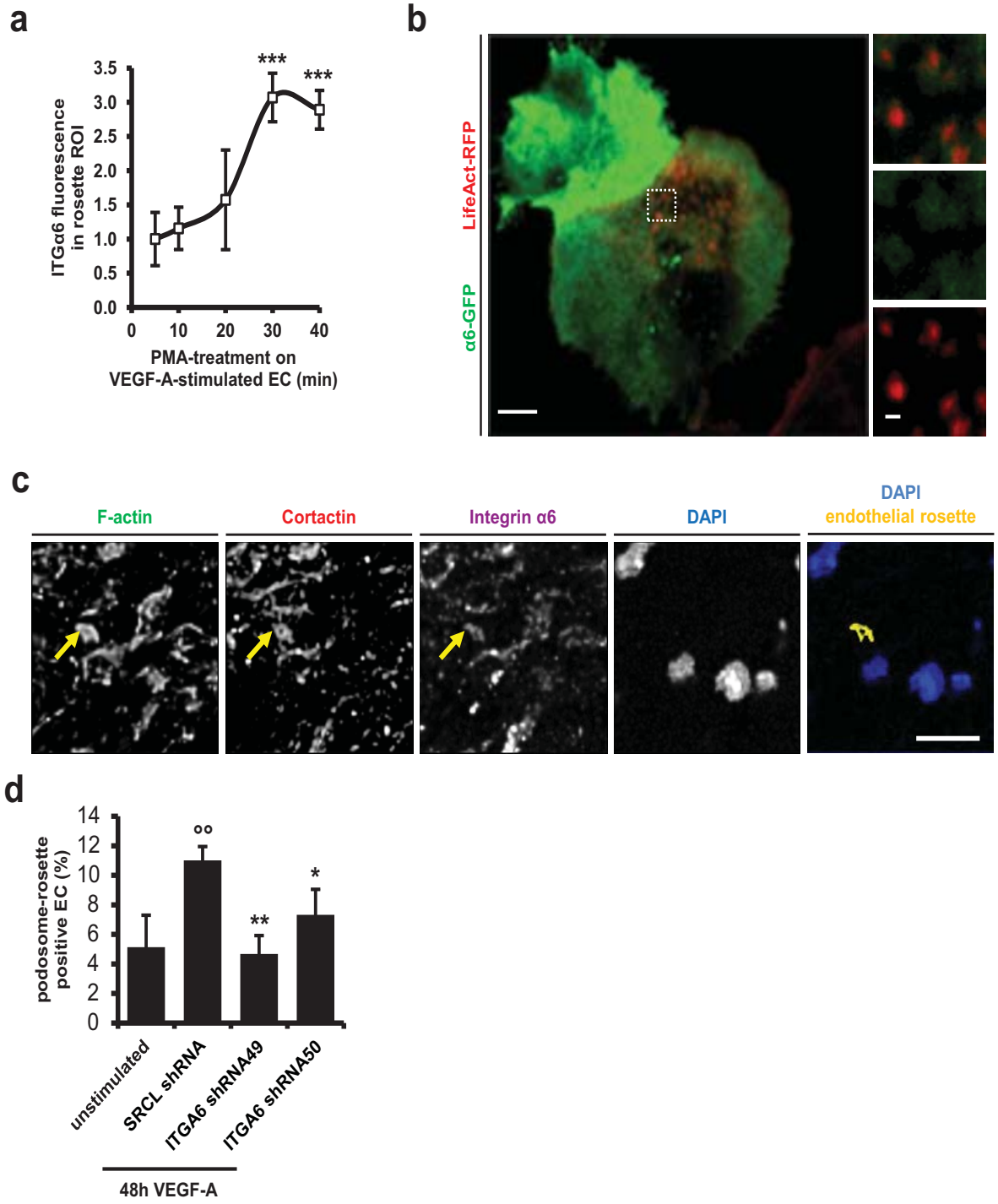

Supplementary Figure 5 Integrin α6 recruitment in endothelial podosomes and integrin α6 silencing in aortic explants. (**a**) Integrin α6 fluorescence quantification in rosettes regions. Rosettes regions were manually selected using co-localization of cortactin and F-actin staining. Mean ± SEM of n = 3 independent experiments in which 30 total cells were analyzed cells per experimental point. (***, P < 0.001 versus *T=0*.) Statistical significance was calculated using paired nonparametric Wilconox test. (**b**) TIRF microscopy of LifeAct-RFP (red) and α6-GFP (green) localization in EC treated with PMA for 15 min. EC were seeded on gelatin-coated glass-bottom dishes. The complete sequence of time-lapse TIRF microscopy is shown in Supplementary Video 2. Scale bar: 20 µm. Zoom of white dotted square is shown in the lower panels. Scale bar: 1 µm. (**c**) Endothelial layer of a 48 h VEGF-A-stimulated aortic explant from Fig. 3f. In yellow, 3D reconstruction of the co-localization channel in podosome rosette. Scale bar: 20 µm. (**d**) Aortic explants were incubated for 48 hours in M199 10% FCS (*unstimulated*) or M199 10% FCS with 30 ng/ml of VEGF-A (*48 h VEGF-A*) plus lentiviruses carrying scramble shRNA (*SCRL shRNA*) and shRNA targeting murine ITGA6 (*shRNA48 and shRNA50*). Graph shows the percentage (%) of podosome-rosettes positive in the endothelial layer of aortic explants, treated and transduced as indicated. Mean ± SEM of n = 3 independent experiments in which 340 total nuclei were analyzed cells per experimental point. (°°, P < 0.01 versus *unstimulated*; *, P < 0.05 versus *SCRL shRNA*; **, P < 0.01 versus *SCRL shRNA*.) Statistical significance was calculated using one-way ANOVA test followed by Bonferroni adjusted post-hoc t-tests.

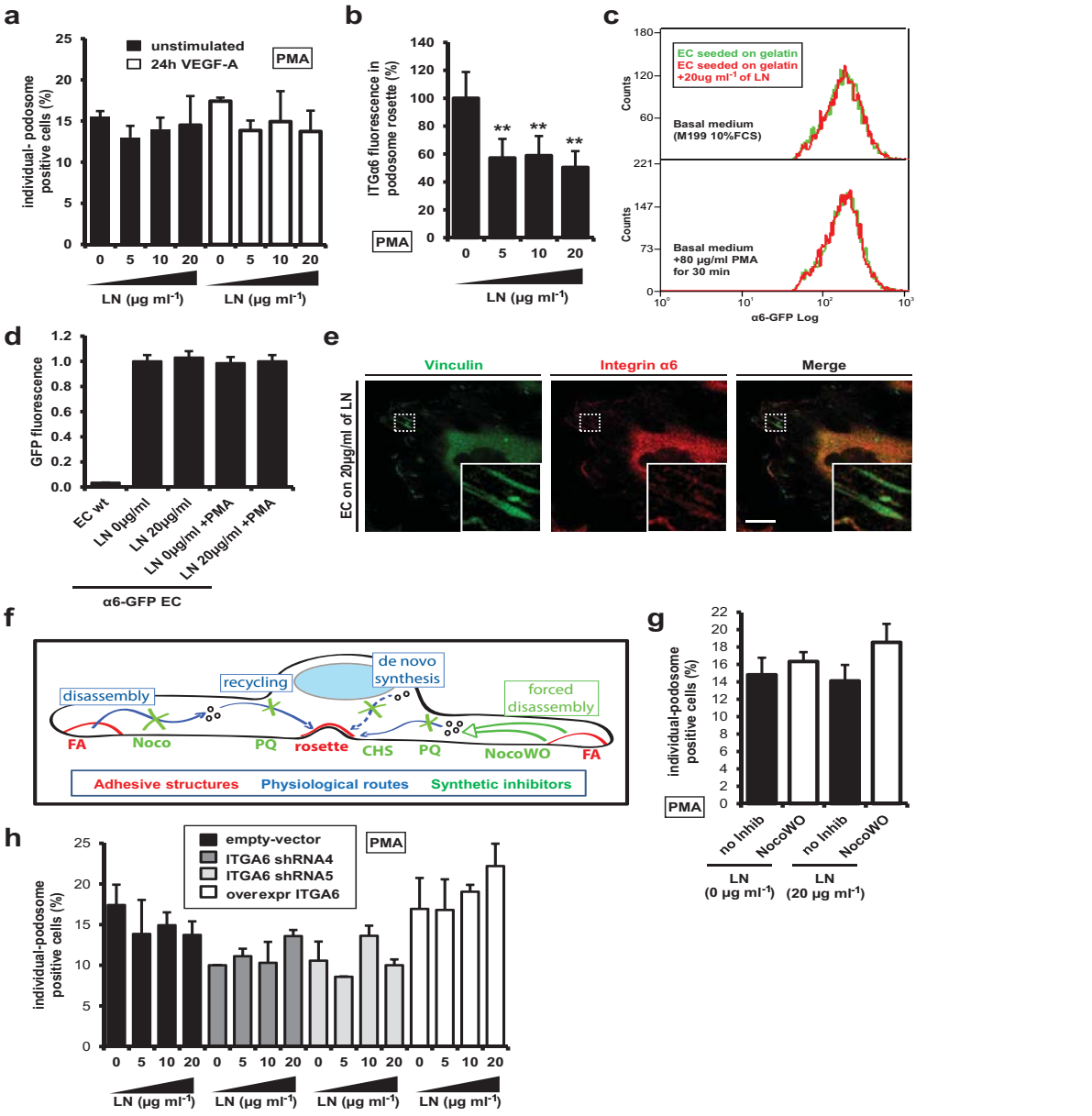

Supplementary Figure 6 Laminin effects on individual podosomes. (**a**) Graph shows the percentages of individual podosome positive EC, stimulated as indicated and seeded on gelatin coated-coverslips with addition of laminin. Percentages of podosome-rosette positive cells in Fig. 4a. Mean ± SEM of n = 3 independent experiments in which 260 total cells were analyzed cells per experimental point. (**b**) Integrin α6 fluorescence quantification in rosettes regions of VEGF-A-stimulated EC. Rosettes ROI were manually selected using the co-localization of cortactin and F-actin staining. Normalized mean ± SEM of n = 3 independent experiments in which 30 cells were quantified per experimental point. (**, $P < 0.01$ versus *LN=0*.) Statistical significance was calculated using one-way ANOVA test followed by Bonferroni adjusted post-hoc t-tests. (**c-d**) Degradation of α6-GFP in PMA-treated EC on laminin. Cytofluorimetric analysis of GFP fluorescence in α6-GFP-transduced EC. EC stimulated as indicated and seeded on gelatin coated-plates with indicated addition of laminin. Mean ± SEM of n = 3 independent experiments in which 10^5 cells were analyzed per experimental point. (**e**) Confocal image of a representative VEGF-stimulated EC seeded on glass-bottom dishes coated with gelatin plus 20 µg/ml of laminin for 2 hours. Inset, of focal adhesion. Scale bar: 20 µm. (**f**) Schematic representation of trafficking model accordingly data shown in Fig. 5a,b. Disassembly of focal adhesions (FA) allows to recruit structural components that are recycled in newly-formed rosettes. Nocodazole (*Noco*) blocks FA disassembly, primaquine (*PQ*) blocks integrin recycling, while *de novo* synthesis blocked by cicloheximide (*CHS*) does not modulate endothelial rosette formation. (**g**) Graph shows the percentages of podosome-rosettes positive EC, seeded on gelatin-coated with indicated laminin addition and PMA-treated with or without nocodazole washout. Percentages of podosome-rosette positive cells in Fig. 5C. Mean ± SEM of n = 3 independent experiments in which 230 cells were analyzed per experimental point. No statistical significance in the modulation of individual podosome was seen. (**h**) Graph shows the percentages of podosome-rosettes positive EC, seeded on gelatin coated-coverslips with indicated addition of laminin. EC were stable-transduced as indicated. Membrane integrin α6 levels in transduced EC are shown in Supplementary Fig. 4d. Percentages of individual-podosome positive cells in Fig. 5d. Mean ± SEM of n = 3 independent experiments in which 420 total cells were analyzed cells per experimental point. No statistical significance in the modulation of individual podosome was seen.

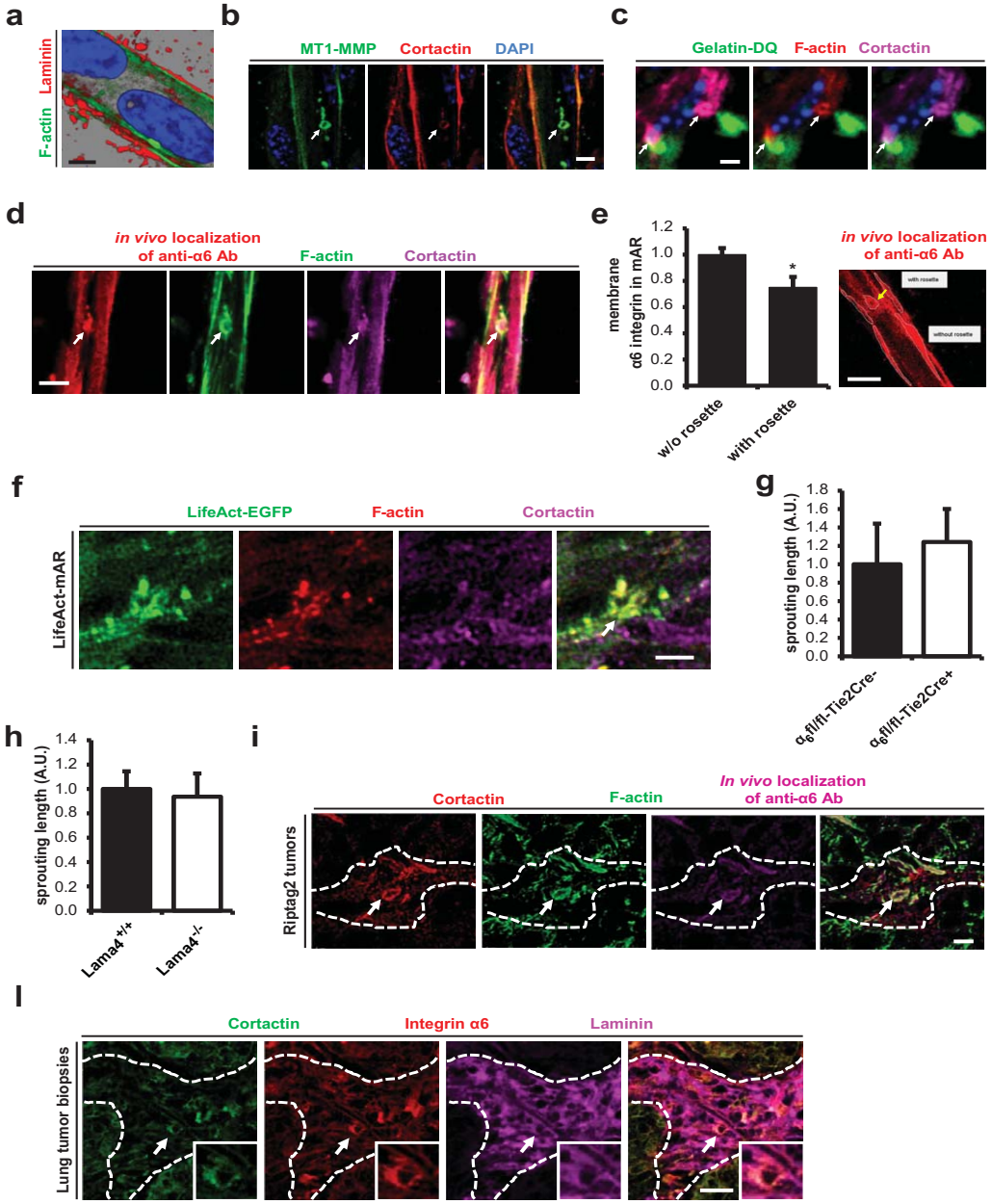

Supplementary Figure 7 Endothelial podosome rosettes in mAR and tumours. (**a**) Self-produced vBM layer – detected as laminin staining – in mAR model. Confocal images of immunostainings for primary Abs as indicated. Scale bar: 5 µm. (**b**) High-magnification confocal images of immunostaining for MT1-MMP in 7-day mAR model. White arrows indicate podosome-rosettes. Scale bar: 5 µm. (**c**) *In situ* zymography in 7-day mAR. Staining for primary Abs as indicated and gelatin-DQ (dye-quenched), *i.e.* degraded gelatin. White arrows indicate podosome-rosettes. Scale bar: 3 µm. (**d**) Rapid accumulation of anti-α6 integrin Ab into focal adhesions and podosome rosettes of mAR detected by secondary anti-rat antibody. Immunostaining with primary Abs as indicated. Scale bar: white arrows indicate 10 µm. Podosome-rosettes. (**e**) Quantification of the localization in membrane of anti-α6 integrin Ab. Normalized mean ± SEM of n = 12 regions of interest (ROI), 4 ROI per mAR for a total of 3 mAR per experimental point. (*, $P < 0.05$ versus *w/o rosette*.) Statistical significance was calculated using unpaired nonparametric Mann-Whitney test. (*right panel*) Schematic representation of the selection of ROIs in panel B. Phalloidin and DAPI stains were used to distinguish the cell edges and phalloidin and cortactin for podosome rosettes. Scale bar: 10 µm. (**f**) Characterization of LifeAct-EGFP mAR endothelial rosettes. Confocal images of immunostainings for primary Abs as indicated. Scale bar: 5 µm. (**g**) Sprout length quantification of capillary-like structures from endothelial α6 null mAR (α_6*fl/fl-Tie2Cre+*.) Normalized mean ± SEM of n = 16 mAR, 4 mAR per mouse from a total of 4 mice. No significative modulation of sprout length was seen. (**h**) Sprout length quantification of capillary-like structures from Laminin α4 KO mAR (*Lama4*$^{-/-}$). Normalized mean ± SEM of n = 8 mAR, 2 mAR per mouse from a total of 4 mice. No significative modulation of sprout length was seen. (**i**) Confocal micrographs of the distribution of immunoreactivity to GoH3 in Riptag2 tumours 10 min after i.v. injection of 25 µg of anti-α6 integrin antibody detected by secondary anti-rat antibody. Immunostaining with primary Abs as indicated. Scale bar: 5 µm. Vessel is delimited by white dotted lines as a guide to the eye; podosome-rosette is indicated by white arrow. (**l**) Confocal micrographs of integrin α6 in podosome rosettes in human tissues. Immunostaining with primary Abs as indicated. Vessel is delimited by white dotted lines as a guide to the eye; podosome-rosettes are indicated by white arrow. Inset, of podosome-rosette. Scale bar: 10 µm.

Supplementary video legends

Supplementary Video 1 – Actin dynamics in endothelial podosome rosettes formation. Time-lapse microscopy of LifeAct-RFP localization in EC treated with PMA for the indicated time. Pseudocolors: TIRF in green and EPI in red. EC were seeded on gelatin-coated glass-bottom dishes. Scale bar: 10 μm.

Supplementary Video 2 – Integrin α6 dynamics in adhesive structures during PMA treatment in EC seeded on laminin-rich substrates or not. Time-lapse TIRF microscopy of LifeAct-RFP (red) and α6-GFP (green) localization in EC treated with PMA for the indicated time. EC were seeded on glass-bottom dishes coated with gelatin plus laminin at indicated concentrations. Scale bar: 15 μm.

Supplementary Video 3 – Focal adhesions and podosome rosettes dynamics during PMA treatment. Time-lapse TIRF microscopy of vinculin-RFP (black) localization in EC. EC were cultured in basal medium and then treated with basal medium plus PMA at the indicated time. EC were seeded on gelatin-coated glass-bottom dishes. Scale bar: 20 μm.

Supplementary Video 4 – 3D reconstruction of endothelial podosome rosettes in angiogenic outgrowths. 3D reconstruction of angiogenic outgrowth from mAR into collagen gel. mAR were stimulated with VEGF-A and FGF-2 for 7 days, then fixed and immunostained. Isosurface of F-actin staining was coloured in gray and endothelial rosettes – co-localization of cortactin and F-actin – in red.

Supplementary Video 5 – Endothelial podosome rosettes in angiogenic outgrowth from LifeAct-EGFP mAR. Xyz-section of time-lapse 2-photon microscopy of angiogenic outgrowths from LifeAct-EGFP mAR, stimulated with VEGF-A and FGF-2. In the video the formation of a 5-6 μm-diameter rosette is evident, followed by a cell protrusion of 14-16 μm of length. Top-left panel is the x-plane, top-right is the z-plane, bottom-left is the y-plane and bottom-right is the image. Scale bar: 20 μm.

Supplementary Video 6 – Branching from endothelial rosettes in LifeAct-EGFP mAR. Time-lapse 2-photon microscopy of angiogenic outgrowths from LifeAct-EGFP mAR, stimulated with VEGF-A and FGF-2. Inset, 3D reconstruction of endothelial podosome rosette of the same video. Scale bar: 50 μm.

Supplementary Video 7 – Dynamical analysis of vessel branching in endothelial ITGA6 KO mAR. Time-lapse phase-contrast microscopy of angiogenic outgrowths from mAR. mAR from WT (α6fl/fl-Tie2Cre-) or endothelial α6 KO (α6fl/fl-Tie2Cre+) mice were stimulated with VEGF-A and FGF-2. Scale bar: 70 μm.

Supplementary Video 8 – Dynamical analysis of vessel branching in Lama4$^{-/-}$ KO mAR. Time-lapse phase-contrast microscopy of angiogenic outgrowths from mAR. mAR from *WT* or Laminin α4 null (*LAMA4 mAR*) mice were stimulated with VEGF-A and FGF-2. Scale bar: 70 μm.

Supplementary Video 9 - Dynamical analysis of vessel branching in mAR into laminin-rich matrices. Time-lapse phase-contrast microscopy of angiogenic outgrowths from mAR into type-I-collagen gel with or without 20 μg/ml of laminin addition. mARs were stimulated with VEGF-A and FGF-2. Scale bar: 70 μm.